AMP-PNP, followed by cross-linking and electron microscopic analysis, were compared with a biochemical binding analysis by equilibrium dialysis, omitting the cross-linking step (Fig. 2). The comparison showed that glutaraldehyde cross-linking under the conditions used in this study measures the occurrence of GroEL:GroES and GroEL:$(GroES)_2$ particles reliably.
22. J. Frank, J. P. Bretaudiere, J. M. Carazo, A. Verschoor, T. Wagenknecht, *J. Microsc.* **150**, 99 (1988).
23. S. Müller, K. N. Goldie, R. Bürki, R. Häring, A. Engel, *Ultramicroscopy* **46**, 317 (1992).
24. According to Azem *et al.* (*15*), 3.5 μM ATP is sufficient for half-maximal formation of GroEL:GroES complexes in the absence of substrate protein, whereas ~400 μM ATP is necessary for the assembly of GroEL:$(GroES)_2$ particles under the appropriate buffer conditions. We found that a constant concentration of 15 μM ATP is required for GroES binding to occur at the half-maximal rate (*27*). Analysis of the dependence of GroEL- and GroES-mediated folding of bovine rhodanese (*4, 10, 14*) on the ATP concentration showed that half-maximal folding activity is achieved at 50 to 100 μM ATP. Significant renaturation is apparent already at 20 μM ATP. The yield of refolding was 20 to 30% higher at 5 mM $Mg^{2+}$ and pH 7.2 than at 50 mM $Mg^{2+}$ and pH 8.0, at which a large fraction of chaperonin complexes are symmetrical in the absence of substrate protein.
25. [$^3$H]GroES was fully functional in chaperonin-mediated protein folding (*4*).
26. M. J. Todd, P. V. Viitanen, G. H. Lorimer, *Science* **265**, 659 (1994).
27. M. K. Hayer-Hartl, J. Martin, F. U. Hartl, *ibid.* **269**, 836 (1995).
28. 6His-N-DHFR is a construct derived from mouse DHFR and contains the sequence Met-$His_6$-Gly-Cys-Gly joined to the $NH_2$-terminus of DHFR by a factor X cleavage site.
29. Unfolded rhodanese was diluted 100-fold to 0.18 μM from 6 M guanidinium chloride and 5 mM dithiothreitol into a solution of 60 nM GroEL in 50 mM tris-HCl (pH 8.0), 50 mM KCl, and 50 mM magnesium acetate. Aggregates were removed by centrifugation and GroES binding to the rhodanese:GroEL complex in the supernatant fraction was measured as in Fig. 2C. Control reactions lacking rhodanese contained an equivalent concentration of guanidinium chloride.
30. It was shown that GroEL can be cross-linked to a folding intermediate of ribulose-1,5-bisphosphate carboxylase-oxygenase (RuBisCO I) and two GroES oligomers, suggesting that substrate polypeptide binds to the outer surface of GroEL (*15*). Such cross-linking, detected by polyacrylamide electrophoresis in tube gels, may indeed have occurred during the extensive incubation of the protein mixture (60 min) with high concentrations of glutaraldehyde at 37°C (*15*). It may be important in this context that RuBisCO I, after dilution from denaturant, aggregates slowly and is potentially available for cross-linking for long periods of time (*26*). In the present study, GroEL:$(GroES)_2$ complexes were not observed in the presence of unfolded proteins with mild glutaraldehyde cross-linking (*21*) and electron microscopy.
31. Studies describing the formation of GroEL:$(GroES)_2$ particles used reaction buffers containing 15 to 50 mM $Mg^{2+}$ at pH 7.5 to 8.0 (*15, 19, 20*). The free $Mg^{2+}$ concentration in the cell is only 1 to 2 mM (*32*) at a total concentration of 10 to 20 mM. At 20 mM free $Mg^{2+}$ and pH 7.5 (*15*) and in the presence of AMP-PNP, ~30 to 50% of GroEL bound two GroES oligomers, as measured by size-exclusion chromatography. At 50 mM $Mg^{2+}$ and pH 8.0 (*20*), close to 100% of GroEL bound two GroES oligomers (Figs. 2 and 3).
32. T. Alatossava, H. Jutte, A. Kuhn, E. Kellenberger, *J. Bacteriol.* **162**, 413 (1985).
33. A. Bremer, C. Henn, A. Engel, W. Baumeister, U. Aebi, *Ultramicroscopy* **46**, 85 (1992).
34. We thank J. Martin for performing the rhodanese refolding experiments. Supported by NIH grant GM 50908, the Swiss National Foundation for Scientific Research (grant 31-32536.91), and the M. E. Müller Foundation of Switzerland.

4 April 1995; accepted 16 June 1995

# Asymmetrical Interaction of GroEL and GroES in the ATPase Cycle of Assisted Protein Folding

Manajit K. Hayer-Hartl, Jörg Martin, F. Ulrich Hartl*

The chaperonins GroEL and GroES of *Escherichia coli* facilitate protein folding in an adenosine triphosphate (ATP)–dependent reaction cycle. The kinetic parameters for the formation and dissociation of GroEL-GroES complexes were analyzed by surface plasmon resonance. Association of GroES and subsequent ATP hydrolysis in the interacting GroEL toroid resulted in the formation of a stable GroEL:ADP:GroES complex. The complex dissociated as a result of ATP hydrolysis in the opposite GroEL toroid, without formation of a symmetrical GroEL:$(GroES)_2$ intermediate. Dissociation was accelerated by the addition of unfolded polypeptide. Thus, the functional chaperonin unit is an asymmetrical GroEL:GroES complex, and substrate protein plays an active role in modulating the chaperonin reaction cycle.

The chaperonins mediate protein folding in the cell by preventing the formation of unproductive associations within and between nonnative polypeptides (*1–3*). GroEL, the chaperonin in *E. coli* cytosol, is a large oligomeric complex composed of two stacked heptameric rings of identical ~58-kD subunits that form a central cavity (*4, 5*). Studies indicate that GroEL binds one molecule of substrate protein within this cavity in a conformation resembling the molten globule (*3, 4, 6–8*). Folding is achieved through cycles of protein release and rebinding that are dependent on ATP hydrolysis (*3, 9*) and regulated by GroES, a single heptameric ring of ~10-kD subunits (*3, 10–12*). Asymmetrical binding of GroES to one end of the GroEL cylinder has been proposed to be a key feature of the reaction, leaving the cavity of one toroid available for the association of substrate protein (*4*). GroES binding is nucleotide-dependent and is thought to exert a negative cooperative effect, preventing the association of a second GroES oligomer with the opposite GroEL toroid (*4, 13*). GroES increases the cooperativity of the GroEL adenosine triphosphatase (ATPase) (*12, 14–16*) and, after ATP hydrolysis, stabilizes the seven interacting GroEL subunits in the adenosine diphosphate (ADP)–bound state (*15*). As a result, the GroEL ATPase is inhibited by 50% (*10*). GroES dissociates after ATP hydrolysis in the uninhibited GroEL toroid (*15, 17*); its association (or reassociation) with a substrate:GroEL complex results in ATP-dependent protein release for folding.

Recently, the electron microscopic observation of symmetrical GroEL:$(GroES)_2$ complexes (*18–20*) has led to several new proposals that differ from the model of chaperonin action outlined above: (i) The symmetrical chaperonin particle was invoked as an obligatory intermediate preceding the step of ATP hydrolysis in the reaction that results in GroES release (*17, 20*). (ii) Substrate protein was proposed to interact with the outer surface of the chaperonin cylinder because symmetrical binding of GroES would prevent access to the GroEL cavity (*19*). (iii) The interaction between GroEL and GroES was claimed to be independent of substrate protein (*17*). We have now analyzed the steps of the chaperonin reaction cycle with kinetic and biochemical methods that allowed us to distinguish between a functional stoichiometry for GroEL:GroES of 1:1 or 1:2.

Complex formation between GroEL and GroES as a function of nucleotide binding was analyzed by surface plasmon resonance (SPR). This technique measures the real-time association and dissociation of protein molecules on a sensor surface and allows precise and highly reproducible estimates of kinetic binding constants (*21*). The kinetic properties of the GroEL-GroES interaction were compared under various conditions. Either GroEL or GroES was functionally immobilized to the sensor surface of the flow cell. Efficient complex formation occurred in the presence of adenine nucleotide and $Mg^{2+}$ (Fig. 1) (*22*). Similar binding parameters were obtained irrespective of whether GroEL or GroES was immobilized (Fig. 1 and Table 1). Thus, covalent coupling to the flow cell per se did not affect the functional properties of these proteins (*23*). SPR response curves for the ADP-dependent binding of increasing concentrations of GroEL to immobilized GroES are shown in Fig. 1A. Association occurred in a monophasic reaction with an apparent rate constant, $k_a$, of ~$4 \times 10^5$ $M^{-1}$ $s^{-1}$ (Table 1). Association may be slower than that in free solution because of the motional restraint of one of the partner molecules. The rate of complex formation in the presence of ATP was approximately three times that in the presence of ADP (Fig. 1B and Table

Howard Hughes Medical Institute and Cellular Biochemistry and Biophysics Program, Memorial Sloan-Kettering Cancer Center, 1275 York Avenue, New York, NY 10021, USA.

*To whom correspondence should be addressed.

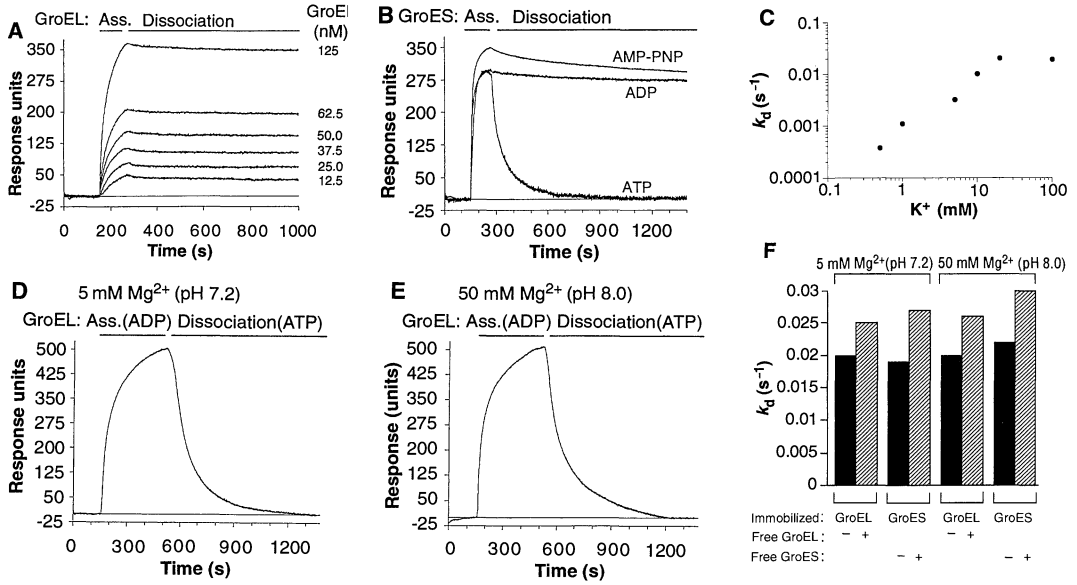


**Fig. 1.** Real-time SPR detection of the interaction between GroEL and GroES. (**A**) Resonance response units (RU) as a function of time (sensorgrams) for the ADP-dependent binding of GroEL to immobilized GroES (300 RU, ~40 μM GroES oligomer in the flow cell) (*36, 38*). Approximately 50% of immobilized GroES was competent to bind GroEL, as determined by titration experiments. The flow cell was equilibrated at 25°C in buffer A [20 mM MOPS-NaOH (pH 7.2), 20 mM KCl, 80 mM NaCl, 5 mM magnesium acetate] containing 0.2 mM ADP [association (Ass.) and dissociation phases], and GroEL was injected in the same buffer (association phase). The buffer flow rate during both phases was 15 μl $min^{-1}$. Higher flow rates did not change the kinetic parameters determined. (**B**) Sensorgrams for the interaction of GroES (240 nM) with immobilized GroEL (5000 RU, ~60 μM in the flow cell) in buffer A containing 0.2 mM ADP, 2 mM ATP, or 2.5 mM AMP-PNP, as indicated. Approximately 80 to 90% of GroEL was competent in GroES binding. (**C**) Observed dissociation rate constants, $k_d$, for the ATP-dependent dissociation of GroEL:ADP:GroES versus the $K^+$ concentration in the buffer. GroEL (125 nM) was injected at 10 μl $min^{-1}$ into a flow cell containing 300 RU of immobilized GroES in buffer B [20 mM MOPS-NaOH (pH 7.2), 5 mM magnesium acetate] containing 100 mM NaCl, 0.5 mM KCl, and 0.2 mM ADP. After the association phase, the same buffer without GroEL was continued for 8 min, followed by a 3-min injection of buffer B containing 2 mM ATP and 0.5 to 100 mM KCl, as well as 100 to 0 mM NaCl to maintain a constant salt concentration. (**D**) Dissociation of GroEL from a preformed GroEL:GroES complex. GroEL (125 nM) was injected into a flow cell containing 300 RU of immobilized GroES in buffer A containing 0.2 mM ADP. After the association phase, buffer A containing 2 mM ATP was injected to observe the dissociation of the complex. (**E**) The same experiment as in (D) was performed in buffer C [50 mM tris-HCl (pH 8.0), 50 mM KCl, 50 mM magnesium acetate] (*20*) containing 0.2 mM ADP during association and 2 mM ATP during dissociation. (**F**) GroES or GroEL was injected into a flow cell containing immobilized GroEL or GroES, respectively, with buffer A or buffer C containing 0.2 mm ADP, as indicated. After the association phase, the respective buffer containing 2 mM ATP was injected either alone or with 2.5 μM GroEL or 20 μM GroES, respectively (*29*). On injection of ATP-containing buffer alone, a fast phase and a slow phase of dissociation were observed. The $k_d$ of the fast phase is plotted (average of three experiments).

1). Given that the GroEL subunits hydrolyze ATP at a rate of ~0.08 $s^{-1}$, GroES associates with ATP-bound GroEL before hydrolysis (*24*), which is also consistent with the observation of rapid GroES binding promoted by the nonhydrolyzable ATP analog adenylyl imidodiphosphate (AMP-PNP) (Fig. 1B).

Spontaneous dissociation of the GroEL:GroES complex formed in the presence of ADP was extremely slow (Fig. 1, A and B). The dissociation rate constant, $k_d$, was ~5 × $10^{-5}$ $s^{-1}$ [half-time ($t_{1/2}$), ~4 hours], which is consistent with the stability of the GroEL:ADP:GroES complex determined in free solution (*16, 17*). In contrast, the complex formed in the presence of ATP dissociated rapidly when ATP-containing buffer was continued after the association phase (Fig. 1B). About 50 to 70% of GroES dissociated from immobilized GroEL with a rate of ~0.02 $s^{-1}$ ($t_{1/2}$, ~30 s), the rest at a rate of approximately half the initial rate (Fig. 1B). This slower rate was attributable to reassociation of GroES with GroEL (Fig. 1F), which became significant as the concentration of unliganded GroEL increased during the dissociation phase. Dissociation of GroES:GroEL was dependent on ATP hydrolysis, because the complex dissociated very slowly in the presence of AMP-PNP ($t_{1/2}$ ~ 40 min). Furthermore, the rate of

**Table 1.** Kinetic parameters for the interaction between GroEL and GroES determined by SPR (*36*). Apparent association ($k_a$) and dissociation ($k_d$) rate constants as well as the dissociation equilibrium constants ($K_d = k_d/k_a$) are means ± SEM of three to six independent experiments. The $k_d$ in the presence of ATP is the fast rate constant observed in the absence of competitor (Fig. 1F) (*29*). SPR measurements (*21*) were performed in buffer A [5 mM $Mg^{2+}$ (pH 7.2)] and in buffer C [50 mM $Mg^{2+}$ (pH 8.0)] with immobilized GroEL or GroES, as described in Fig. 1, at a series of concentrations of free analyte of 12.5 to 125 nM (GroEL) or 60 to 600 nM (GroES). The concentrations of ATP, ADP, and AMP-PNP were 2, 0.2, and 2.5 mM, respectively. Association rate data were fitted to the exponential equation $R_t = [Ck_a R_{max}/(Ck_a + k_d)][1 - e^{-(Ck_a + k_d)t}]$ with nonlinear least-squares analysis software (Igor; WaveMetrics). The use of this pseudo–first order interaction is appropriate because the analyte concentration in the 60-nl flow cell is approximately constant during the association phase, given the high flow rates of analyte solution and the small amounts of immobilized ligand. $R_t$, resonance response units (RU) at time $t$ (seconds); C, concentration of the injected analyte (molar); $R_{max}$, maximum RU possible if analyte bound 100% of immobilized ligand. The residual plots of the difference between the actual data and the predicted data were <5 RU in magnitude. Dissociation data were fitted with either a single- or double-exponential model as described in the Pharmacia Biosensor BIA evaluation software 2.0 and by O'Shannessy *et al.* (*37*).

| Nucleotide | Immobilized ligand | *n* | $k_a$ ($10^5$ $M^{-1}$ $s^{-1}$) | $k_d$ ($10^{-4}$ $s^{-1}$) | $K_d$ (nM) |
|---|---|---|---|---|---|
| | | | *5 mM $Mg^{2+}$ (pH 7.2)* | | |
| ADP | GroEL | 6 | 3.6 ± 0.5 | 0.65 ± 0.10 | 0.2 ± 0.02 |
| ADP | GroES | 6 | 4.5 ± 2.0 | 0.39 ± 0.05 | 0.1 ± 0.03 |
| ATP | GroEL | 10 | 12 ± 5 | 200 ± 20 | 16.7 ± 3.0 |
| ATP | GroES | 12 | 11 ± 5 | 190 ± 20 | 17.3 ± 4.0 |
| AMP-PNP | GroEL | 4 | 3.6 ± 1.0 | 2.9 ± 1.0 | 0.8 ± 0.02 |
| AMP-PNP | GroES | 5 | 6.8 ± 2.0 | 2.8 ± 1.0 | 0.4 ± 0.03 |
| | | | *50 mM $Mg^{2+}$ (pH 8.0)* | | |
| ADP | GroEL | 6 | 1.2 ± 0.5 | 1.2 ± 0.3 | 1.0 ± 0.3 |
| ADP | GroES | 8 | 2.4 ± 1.0 | 3.0 ± 1.0 | 1.3 ± 0.5 |
| ATP | GroEL | 12 | 11 ± 2 | 200 ± 20 | 18.2 ± 1.0 |
| ATP | GroES | 6 | 9 ± 2 | 200 ± 20 | 22.2 ± 2.0 |
| AMP-PNP | GroEL | 5 | 5.0 ± 2.0 | 4.2 ± 1.0 | 0.8 ± 0.05 |
| AMP-PNP | GroES | 4 | 2.7 ± 0.3 | 3.8 ± 0.5 | 1.4 ± 0.03 |

ATP-dependent dissociation was dependent on the presence of $K^+$ in the solution, reflecting the known $K^+$ requirement for ATP hydrolysis by GroEL (*10*) (Fig. 1C). The ATP hydrolysis that resulted in GroES dissociation must have occurred in the GroEL toroid opposite GroES, because the seven subunits of the GroES-associated toroid were stabilized in the ADP state (*15*), consistent with the 50% inhibition of the GroEL ATPase by GroES (*10, 16*).

It was recently suggested that the ATP hydrolysis–dependent dissociation of the GroEL:GroES complex depends on the formation of a symmetrical GroEL:$(GroES)_2$ intermediate (*17, 20*). SPR analysis allowed us to test specifically whether formation of symmetrical complexes is obligatory for the GroEL ATPase cycle. GroES dissociated from GroEL with full efficiency at ATP concentrations of 20 to 50 μM, at which symmetrical chaperonin particles are not detectable (*19, 25*). When high concentrations of GroES were injected into the SPR flow cell in a buffer (pH 8.0, 50 mM $Mg^{2+}$) that promotes the stable association of two GroES oligomers per GroEL (*13*), an increase in the rate of ATP-dependent dissociation of GroEL:GroES was not apparent (Table 1), further arguing against a critical role of GroEL:$(GroES)_2$ complexes in this step of the reaction cycle (*26*). At 50 mM $Mg^{2+}$ and pH 8.0, the stability of the GroEL:ADP:GroES complex was reduced by a factor of 10 (Table 1). High $Mg^{2+}$ concentrations affect the intertoroidal interactions in the GroEL oligomer (*27*), apparently resulting in a functional uncoupling of the two heptameric rings (*13*).

To establish definitively whether the ATP hydrolysis–dependent dissociation of GroEL:GroES required the interaction of GroEL with a second GroES (*17*), we took advantage of the fact that GroES binds to GroEL with strict 1:1 stoichiometry in the presence of ADP (*13, 18–20*). The GroEL:ADP:GroES complex was first generated by binding GroEL to immobilized GroES. Subsequently, the ADP- and GroEL-containing buffer was exchanged by injecting ATP-containing buffer into the flow cell of the SPR apparatus (Fig. 1D) (*28*). Complete release of bound GroEL was observed with the same kinetics apparent when ATP was present throughout. If the interaction of a second GroES was necessary for each round of GroES release, either no or only inefficient release of GroEL would be expected in this experiment. Furthermore, according to Todd *et al.* (*17*), a second GroES functions catalytically in triggering the step of ATP hydrolysis that leads to GroES discharge from the opposite GroEL toroid. As a result, the second GroES remains associated with GroEL in the ADP state. In the absence of free GroES under the conditions in Fig. 1, D to F, a GroEL:GroES complex would have to contact another immobilized GroES to allow formation of a GroEL:$(GroES)_2$ structure. GroEL would then be retained on the surface of the flow cell by cycling between two immobilized GroES rings. The observation of rapid and complete dissociation of the asymmetrical chaperonin complex therefore excludes the requirement for a second GroES in the release mechanism.

The rate of ATP-mediated GroEL release from immobilized GroES remained unchanged when dissociation was analyzed at 50 mM $Mg^{2+}$ and pH 8.0, conditions under which symmetrical GroES binding is readily observed in the presence of ATP or AMP-PNP (*13*) (Fig. 1E). Consistent with this observation, injecting free GroES together with ATP during dissociation increased the fast rate of GroEL release only moderately (Fig. 1F) (*29*). At the same time, rebinding of GroEL to immobilized GroES was prevented because a single dissociation rate constant was observed. This effect was not apparent at catalytic concentrations of free GroES and was maximal at high GroES concentrations close to those of the GroEL:GroES complex in the flow cell. It was also independent of whether conditions favoring the formation of GroEL:$(GroES)_2$ structures were used (Fig. 1F). Similarly, injecting free GroEL increased the rate of GroES release when GroEL was immobilized (*29*). Apparently, free GroES acted by inhibiting GroEL rebinding to immobilized GroES rather than by specifically accelerating GroEL:GroES dissociation.

The GroEL oligomer hydrolyzed ~30 ATP molecules per minute in the presence

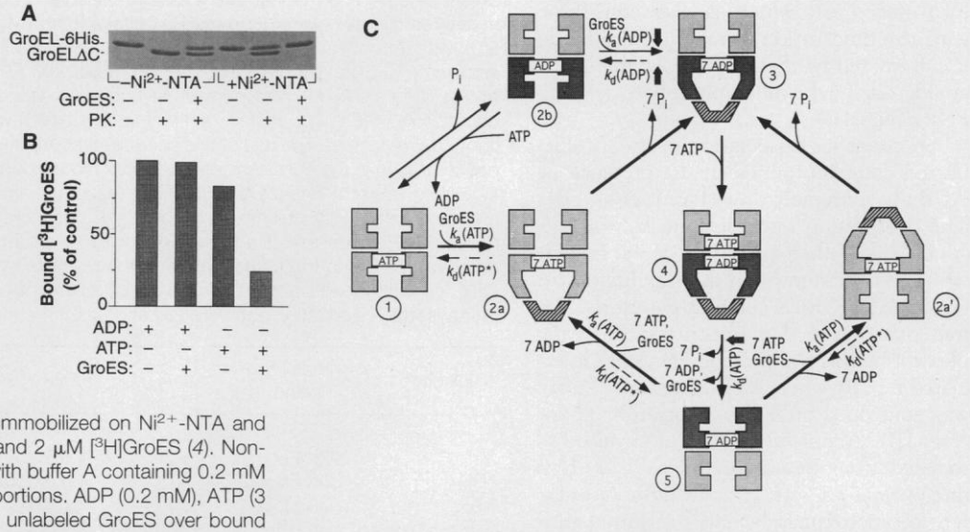


**Fig. 2.** Release and rebinding of GroES to the same GroEL toroid during the reaction cycle. (**A**) Protection from proteolysis of immobilized GroEL-6His after binding of GroES. COOH-terminally His-tagged GroEL (0.12 μM) (*39*), either free in solution or immobilized on $Ni^{2+}$-NTA, was incubated for 15 min with 0.6 μM GroES and 1 mM ADP in buffer A, and then treated with proteinase K (PK) (10 μg/ml) at 25°C for 10 min, as indicated. Digestion was terminated with 1 mM phenylmethylsulfonyl fluoride, and samples were boiled in SDS sample buffer containing 200 mM imidazole and analyzed by SDS–polyacrylamide gel electrophoresis and Coomassie blue staining. GroEL-ΔC, COOH-terminally clipped GroEL-6His. (**B**) GroEL-6His (0.12 μM) was immobilized on $Ni^{2+}$-NTA and incubated in buffer A containing 1 mM ADP and 2 μM [$^3$H]GroES (*4*). Nonbound [$^3$H]GroES was removed by washing with buffer A containing 0.2 mM ADP, and the sample was then split into four portions. ADP (0.2 mM), ATP (3 mM), or a 10-fold molar excess (1.25 μM) of unlabeled GroES over bound [$^3$H]GroES was added as indicated. After 5 min, hexokinase (30 U/ml) and 25 mM glucose were added, followed by washing of the $Ni^{2+}$-NTA–adsorbed chaperonin complexes with buffer A containing 1 mM ADP. Bound [$^3$H]GroES was determined by liquid scintillation spectroscopy and is plotted as a percentage of the amount of [$^3$H]GroES initially bound to GroEL. (**C**) Model for the nucleotide-dependent interaction of GroEL and GroES. GroEL is shown as a vertical cut through the cylinder, reflecting the three-domain structure of the subunits (*7*). GroES binding changes the conformation of the interacting GroEL subunits, thereby increasing the volume of the GroEL cavity (*8*). Nucleotide binding to GroES (*15*) is not shown because its functional significance is unclear. The rates for association and dissociation of GroEL and GroES, as well as the direction of their changes on binding of unfolded polypeptide to GroEL, are indicated (gray arrowheads); $k_{cl}$ (ATP) and $k_{cl}$ (ATP*) were measured in the presence of ATP and AMP-PNP, respectively (Table 1). Free GroEL binds up to seven molecules of ATP (intermediate **1**) or ADP (**2b**) (*32*), followed by the assymmetrical association of GroES with the nucleotide-bound ring (**2a** or **2b** to **3**). Between intermediates **2a**′ and **3**, GroEL:GroES is rotated by 180°. $P_i$, inorganic phosphate.

of GroES (~0.04 molecule of ATP per second per subunit) (*24*), in good agreement with the observed rate for the ATP hydrolysis–dependent dissociation of GroEL:GroES. The movement of GroES between different GroEL:GroES complexes would be limited by this rate of ATP hydrolysis. Thus, a "catalytic" function of a second GroES (*17*) does not explain the efficient ATP-dependent release of GroES under conditions in which GroEL:$(GroES)_2$ complexes are not significantly populated (*13*) or GroEL and GroES oligomers are present at only 1:1 stoichiometry.

To investigate whether GroES could rebind to the same GroEL toroid from which release occurred in the preceding round of ATP hydrolysis, or whether GroES must reassociate with the opposite toroid, we took advantage of the observation that binding of GroES protects the seven interacting GroEL subunits from cleavage by proteinase K (*4, 15*). Proteinase K otherwise removes the 16 COOH-terminal amino acid residues that protrude into the central cavity of the chaperonin cylinder as flexible tails (*5, 30*). A six-histidinyl-tagged version of GroEL (GroEL-6His) was generated (*31*), with the tag at the COOH-terminus of the GroEL subunits. The extended COOH-terminal segments were accessible so as to allow immobilization of the protein on $Ni^{2+}$–nitrilotriacetic acid (NTA) agarose in a defined topology, with only one end of the GroEL cylinder exposed to bind GroES. Whereas proteinase K treatment of free GroEL-6His in the absence of GroES resulted in the COOH-terminal truncation of all 14 subunits, only half the subunits were cleaved by the protease in the presence of GroES and ADP (Fig. 2A). Binding to $Ni^{2+}$-NTA beads afforded the same protection against proteolysis as GroES association. Addition of GroES and ADP to immobilized GroEL-6His resulted in protection of all GroEL subunits.

When [$^3$H]GroES was bound to immobilized GroEL-6His in the presence of ADP, it was not exchangeable on addition of excess unlabeled GroES (Fig. 2B), reflecting the high stability of GroEL:ADP:[$^3$H]GroES. In contrast, when a GroEL:ADP:[$^3$H]GroES complex was first formed on $Ni^{2+}$-NTA beads and then challenged with ATP and unlabeled GroES, [$^3$H]GroES was efficiently eluted, confirming that binding of a second GroES was not required for the release step. Significantly, only little [$^3$H]GroES was recovered in the supernatant of the $Ni^{2+}$-NTA beads after incubation with Mg-ATP alone. Unlike the situation in the SPR experiments, in the experiments with immobilized GroEL-6His efficient re-formation of GroEL:GroES occurred before the molecules could be physically separated. Consequently, ATP-dependent release of [$^3$H]GroES was observed only by exchange with unlabeled GroES. Thus, the same GroEL toroid from which GroES dissociated in the preceding round of ATP hydrolysis is competent to rebind GroES in the subsequent ATPase cycle. Neither the dissociation of the asymmetrical chaperonin complex nor its reassociation requires the transient interaction of GroES with both ends of the GroEL cylinder.

Our results describe the ATPase cycle for the interaction of GroEL and GroES (Fig. 2C). In the presence of GroES, ATP hydrolysis by GroEL is highly cooperative at the level of the heptameric rings (*12, 14, 16*). The two GroEL toroids are allosterically connected so that one ring is in the ATP state and the other in the ADP state, corresponding to low- and high-affinity states for polypeptide binding, respectively. This asymmetry, introduced by binding of ATP to only one GroEL toroid (*32*), is maintained by coupling ATP hydrolysis in one ring to the dissociation of ADP and GroES from the opposite ring (Fig. 2C from intermediates **3** to **4** to **5**). GroES associates predominantly with the ATP-bound GroEL toroid (Fig. 2C, from **1** to **2a**) (*24*). A first round of ATP hydrolysis then results in the association of GroES with the interacting GroEL ring in the ADP-bound state (*15*). This complex is very stable and is resolved only by ATP hydrolysis in the opposite toroid (Fig. 1, B and C), resulting in the exchange of tightly bound ADP for ATP and in GroES release. GroES then rebinds either to the same GroEL toroid from which dissociation occurred in the preceding round of ATP hydrolysis (Fig. 2, A and B) or to the alternative toroid (Fig. 2C, from **5** to **2a′** to **3**). Partitioning of GroES between

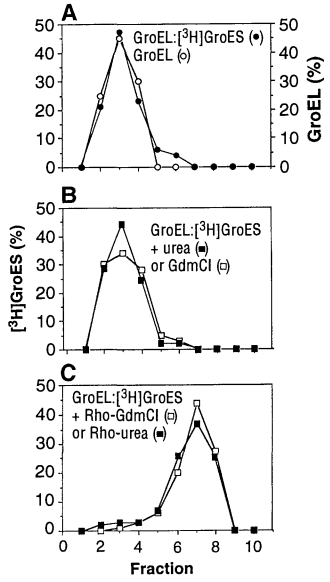


**Fig. 3.** Substrate protein–induced dissociation of GroEL:GroES complexes detected by size-exclusion chromatography. (**A**) Fractionation of GroEL and GroEL:[$^3$H]GroES complexes. GroEL (0.1 μM) was incubated for 15 min at 25°C in a solution containing 20 mM MOPS (pH 7.2), 10 mM KCl, 90 mM NaCl, 5 mM $MgCl_2$, and 1 mM dithiothreitol (DTT), with or without 0.1 μM [$^3$H]GroES. The sample was then applied to a Sephacryl S300-HR (Pharmacia) column (0.5 by 6 cm) that had been equilibrated in the same buffer. Fractions (130 μl) were analyzed by SDS–polyacrylamide gel electrophoresis, fluorography, and laser densitometry. (**B**) Effects of denaturants on the stability of GroEL:[$^3$H]GroES complexes. A 10-fold molar excess of unlabeled GroES (1 μM) over GroEL was added to GroEL:[$^3$H]GroES complexes formed as in (A) to allow for potential exchange of labeled by unlabeled GroES. After addition of 40 mM guanidinium chloride (GdmCl) and 33 μM DTT, or 60 mM urea and 38 μM DTT, the reaction mixtures were immediately applied to Sephacryl S300-HR columns and analyzed as in (A). (**C**) Displacement of [$^3$H]GroES from GroEL by addition of unfolded substrate protein in the presence of excess unlabeled GroES. Experiments were performed essentially as in (B), but unfolded rhodanese (0.3 μM, final concentration) (Rho) was added in either urea or GdmCl [rhodanese was denatured by incubation for 1 hour in 6 M GdmCl and 5 mM DTT, or in 8 M urea and 5 mM DTT (*3, 15, 40*)]. Final concentrations of denaturants as in (B).

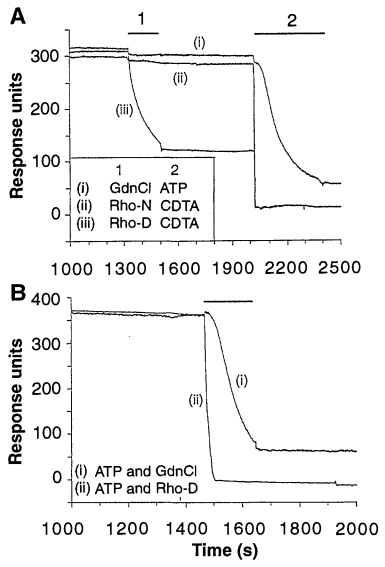


**Fig. 4.** Effect of unfolded rhodanese on the dissociation of GroEL:GroES detected by SPR. (**A**) GroEL was injected into a flow cell containing immobilized GroES (370 RU) with buffer A containing 0.2 mM ADP. Approximately 300 RU of GroEL was bound. After the association phase, buffer flow was continued for 10 min (approximately the last 5 min are shown). Subsequently, buffer A containing 0.2 mM ADP and either 60 mM GdmCl (trace i), 0.45 μM native rhodanese (Rho-N) (trace ii), or 0.45 μM unfolded rhodanese and 60 mM GdmCl (Rho-D) (trace iii) (*40*) was injected for 3 min at a flow rate of 10 μl $min^{-1}$. Horizontal bar 1 indicates the injection time. After injection of buffer A containing 0.2 mM ADP for 10 min, buffer A containing either 2 mM ATP (trace i) or 5 mM CDTA (traces ii and iii) was injected for 6 min at 5 μl $min^{-1}$. Horizontal bar 2 indicates injection time. (**B**) GroEL was bound to immobilized GroES as in (A). After washing the flow cell with buffer A containing 0.2 mM ADP, buffer A containing either 2 mM ATP and 60 mM GdmCl (trace i) or 2 mM ATP and 0.45 μM unfolded rhodanese (containing 60 mM GdmCl) (trace ii) was injected (horizontal bar) for 3 min at 10 μl $min^{-1}$.

both GroEL rings has been observed in the presence of ATP (*15*). Thus, 14 ATP molecules are hydrolyzed in a complete reaction cycle of GroES release and rebinding. The rate of ATP hydrolysis by GroEL in the presence of GroES (*24*) corresponds closely to the observed rate for the ATP-dependent dissociation of GroEL:GroES (Fig. 1E and Table 1), identifying ATP hydrolysis as the rate-limiting step in the cycle. Throughout the reaction, the asymmetrical GroEL:GroES complex is the functional unit (Fig. 1, D to F, and Fig. 2, A and B), thus allowing for facile access of substrate protein to the chaperonin cavity. Symmetrical GroEL:$(GroES)_2$ complexes are significantly populated only in the absence of substrate protein and under specific salt and pH conditions (*13*).

Does unfolded polypeptide substrate actively modify the kinetic parameters of the GroEL-GroES interaction? We analyzed the effect of substrate protein on the stability of the GroEL:GroES complex. When [$^3$H]GroES (*4*) was first bound to GroEL in the presence of ADP, it was not exchangeable from the complex by an excess of unlabeled GroES, as determined by size-exclusion chromatography (Fig. 3A). In contrast, when denatured rhodanese was added, [$^3$H]GroES was efficiently exchanged and fractionated as the free protein (Fig. 3C). Addition of denaturant alone, carried over with the unfolded rhodanese, was without detectable effect (Fig. 3B) (*33*). Substrate protein likely exerts this effect by binding into the central cavity of the GroEL toroid that is not occupied by GroES (*8*, *13*).

The rate for the substrate-induced dissociation of GroEL:GroES was measured by SPR. Unfolded rhodanese was injected into a flow cell containing immobilized GroES in a complex with ADP-bound GroEL. About 60% of GroEL was released at an initial rate comparable to that measured in the presence of ATP (Fig. 4A). Incomplete release may be explained by rebinding of the GroEL:ADP:rhodanese complex to GroES (*15*). In contrast, GroEL remained bound to GroES when an equivalent concentration of denaturant or native rhodanese was injected. The simultaneous exposure of GroEL:ADP:GroES to unfolded rhodanese and ATP resulted in the complete dissociation of GroEL from GroES at a rate of approximately 0.1 $s^{-1}$ ($t_{1/2}$, ~7 s), about three times the rate of dissociation in the presence of ATP alone (Fig. 4B). More rapid dissociation was apparent only on injection of the $Mg^{2+}$ chelator (CDTA) cyclohexane diamine tetraacetic acid, which most likely results in the removal of the tightly bound nucleotide that stabilizes the GroEL:GroES complex (Fig. 4A).

We propose that binding of unfolded polypeptide accelerates the dissociation of the GroEL:GroES complex by (i) stimulating ATP hydrolysis in the non–GroES-bound toroid of GroEL (Fig. 2C, from **4** to **5**) and (ii) facilitating the release of tightly bound ADP from the GroES-bound toroid in a manner independent of ATP hydrolysis (Fig. 2C, from **3** to **2b**) (*15*). A continuous stimulation of the GroEL ATPase by both chemically denatured (*3*) and permanently unfolded polypeptide substrates (*3*, *4*, *12*) has been described. Interaction with substrate would thus serve to reset the GroEL-GroES reaction cycle, allowing the binding (or rebinding) of ATP and GroES to the GroEL complex, followed by ATP hydrolysis for protein release and folding (*34*). GroES may exert its effect on substrate release by interacting with the free toroid of the GroEL:polypeptide complex. Alternatively, GroES may preferentially bind (or rebind) to the toroid that contains the substrate protein (Fig. 2C, form **4** to **5** to **2a′**) (*15*), possibly resulting in the displacement of polypeptide into the GroEL cavity for (partial) folding and subsequent polypeptide release from the cavity on GroES dissociation (*35*). Whichever mechanism predominates, it is unlikely that symmetrical chaperonin complexes play a critical role in chaperonin-mediated protein folding, because their formation and polypeptide binding by GroEL are mutually exclusive (*13*).

## REFERENCES AND NOTES


1. J. Ellis, *Nature* **328**, 378 (1987); S. J. Landry and L. M. Gierasch, *Annu. Rev. Biomol. Struct.* **23**, 645 (1994); J. P. Hendrick and F. U. Hartl, *Annu. Rev. Biochem.* **62**, 349 (1993).
2. S. M. Hemmingsen *et al.*, *Nature* **333**, 330 (1988); M. Y. Cheng *et al.*, *ibid.* **337**, 620 (1989); J. Ostermann, A. L. Horwich, W. Neupert, F. U. Hartl, *ibid.* **341**, 125 (1989); P. Goloubinoff, J. T. Christeller, A. A. Gatenby, G. H. Lorimer, *ibid.* **342**, 884 (1989); A. A. Laminet, T. Ziegelhoffer, C. Georgopoulos, A. Plückthun, *EMBO J.* **9**, 2315 (1990).
3. J. Martin *et al.*, *Nature* **352**, 36 (1991).
4. T. Langer, G. Pfeifer, J. Martin, W. Baumeister, F. U. Hartl, *EMBO J.* **11**, 4757 (1992).
5. H. R. Saibil *et al.*, *Curr. Biol.* **3**, 265 (1993); K. Braig *et al.*, *Nature* **371**, 578 (1994).
6. M. K. Hayer-Hartl, J. J. Ewbank, T. E. Creighton, F. U. Hartl, *EMBO J.* **13**, 3192 (1994); C. V. Robinson *et al.*, *Nature* **372**, 646 (1994); R. Zahn and A. Plückthun, *J. Mol. Biol.* **242**, 165 (1994); R. Zahn, C. Spitzfaden, M. Ottiger, K. Wüthrich, A. Plückthun, *Nature* **368**, 261 (1994).
7. K. Braig, M. Simon, F. Furuya, J. F. Hainfeld, A. L. Horwich, *Proc. Natl. Acad. Sci. U.S.A.* **90**, 3978 (1993).
8. S. Chen *et al.*, *Nature* **371**, 261 (1994).
9. J. S. Weissman, Y. Kashi, W. A. Fenton, A. L. Horwich, *Cell* **78**, 693 (1994).
10. P. V. Viitanen *et al.*, *Biochemistry* **29**, 5664 (1990).
11. M. Schmidt, J. Buchner, M. J. Todd, G. H. Lorimer, P. V. Viitanen, *J. Biol. Chem.* **269**, 10304 (1994).
12. G. S. Jackson *et al.*, *Biochemistry* **32**, 2554 (1993).
13. A. Engel *et al.*, *Science* **269**, 832 (1995).
14. T. E. Gray and A. R. Fersht, *FEBS Lett.* **292**, 254 (1991); E. S. Bochkareva and A. S. Girshovich, *J. Biol. Chem.* **267**, 25672 (1992).
15. J. Martin, M. Mayhew, T. Langer, F. U. Hartl, *Nature* **366**, 228 (1993); J. Martin, S. Geromanos, P. Tempst, F. U. Hartl, *ibid.*, p. 279.
16. M. J. Todd, P. V. Viitanen, G. H. Lorimer, *Biochemistry* **32**, 8560 (1993).
17. ———, *Science* **265**, 659 (1994).
18. O. Llorca, S. Marco, J. L. Carrascosa, J. M. Valpuesta, *FEBS Lett.* **345**, 181 (1994).
19. A. Azem, M. Kessel, P. Goloubinoff, *Science* **265**, 653 (1994).
20. M. Schmidt *et al.*, *ibid.*, p. 656.
21. U. Jonsson *et al.*, *Biotechniques* **11**, 620 (1991); L. G. Fagerstam, A. Frostell-Karlsson, R. Karlsson, B. Persson, I. Ronnberg, *J. Chromatogr.* **597**, 397 (1992); S. C. Schuster, R. V. Swanson, L. A. Alex, R. B. Bourret, M. I. Simon, *Nature* **365**, 343 (1993).
22. In the absence of nucleotide, a constant flow of GroEL or GroES past the sensor surface containing the respective partner molecule did not change the SPR response.
23. Half-maximal rates of association were measured at concentrations of 15 μM ATP, 50 μM ADP, and 500 μM AMP-PNP, consistent with the binding affinities of GroEL for these nucleotides (*12*).
24. ATP hydrolysis by GroEL was measured with [$\gamma^{-32}$P]ATP as described (*10*). On the basis of an observed rate constant for the ATP-dependent association of GroEL and GroES of $>10^6$ $M^{-1}$ $s^{-1}$ (Table 1), complex formation would be more rapid than ATP hydrolysis at concentrations of GroEL and GroES of >50 nM. The cellular concentration ratio of ATP:ADP is ~10:1, and the concentration of GroEL and GroES in the cytosol is in the range of 3 to 5 μM.
25. Analysis of the dependence of GroEL- and GroES-mediated folding of rhodanese (*3*, *15*) on ATP concentration showed that half-maximal folding activity is achieved at 50 to 100 μM ATP. Significant renaturation is already apparent at 20 μM ATP. The yield of refolding at 5 mM $Mg^{2+}$ and pH 7.2 was 120 to 130% of that at 50 mM $Mg^{2+}$ and pH 8.0, under which conditions symmetrical chaperonin complexes form in the absence of substrate (*13*).
26. A 20 to 30% increase in GroES binding to immobilized GroEL was measured in the presence of AMP-PNP at pH 8.0 and 50 mM $Mg^{2+}$, relative to binding at pH 7.2 and 5 mM $Mg^{2+}$ (*13*). Formation of GroEL:$(GroES)_2$ complexes in the SPR apparatus should also occur when GroEL is first bound to immobilized GroES in the presence of AMP-PNP and subsequently free GroES is injected with AMP-PNP; however, a significant increase in SRP response units was not observed because of insufficient sensitivity of the instrument.
27. A. Azem, S. Diamant, P. Goloubinoff, *Biochemistry* **33**, 6671 (1994).
28. The same result was obtained when, after the association phase and prior to injecting ATP-containing buffer, the flow cell was extensively washed with ADP-containing buffer (Figs. 1C and 4).
29. The rate increase of ~30% for the dissociation of GroEL:GroES observed after injection of free GroES or GroEL (Fig. 1F) probably reflects an underestimation of the fast dissociation rate in the absence of free ligand as a competitor of rebinding. Lower concentrations of GroEL (2.5 μM; 5 μM GroES binding sites) than GroES were injected together with ATP in the experiment shown in Fig. 1F to avoid the accumulation of ADP.
30. The function of the COOH-terminal 16-residue segment of GroEL is unknown. The removal or extension of this segment does not compromise the functional properties of GroEL (*4*).
31. GroEL-6His was functional in mediating ATP- and GroES-dependent protein folding.
32. E. S. Bochkareva and A. S. Girshovich, *J. Biol. Chem.* **269**, 23869 (1994).
33. The GroEL:ADP:GroES complex was stable in buffer A containing 0.2 mM ADP and up to 100 mM guanidinium chloride (GdmCl), as determined by SPR. However, the complex readily dissociated when exposed to these concentrations of GdmCl in the absence of ADP. The GroEL:GroES complex was previously shown to be sensitive to GdmCl in the absence of free ADP, but stabilized by ADP addition [M. J. Todd and G. H. Lorimer, *J. Biol. Chem.* **270**, 5388 (1995)]. We conclude that the ability of unfolded polypeptide to accelerate the dissociation of the asymmetrical GroEL:GroES complex is most reliably observed at low concentrations of denaturant and in the presence of free nucleotide, either by measuring the exchange of labeled by unlabeled GroES or by SPR analysis.

34. Binding of GroES to a GroEL:polypeptide complex is more rapid in the presence of ATP than ADP (M. K. Hayer-Hartl, unpublished observation).
35. F. U. Hartl, *Nature* **371**, 557 (1994).
36. SPR experiments were performed with the BIAcore apparatus (Pharmacia Biosensor). All protein immobilization was performed at 25°C in buffer A at 0.25 μM GroES and 0.06 μM GroEL. The carboxylated dextran matrix of the 60-nl flow cell (CM5 research grade) was first activated with 1-ethyl-3-(3-dimethylaminopropyl) carbodiimide and *N*-hydroxysuccinimide to allow the subsequent cross-linking of injected protein through primary amine groups (*21*). After cross-linking, the reactive groups were blocked by injection of 1 M ethanolamine (pH 8.5).
37. D. J. O'Shannessy, M. Brigham-Burke, K. K. Soneson, P. Hensley, I. Brooks, *Anal. Biochem.* **212**, 457 (1993).
38. GroEL and GroES proteins were isolated from overproducing strains of *E. coli* as described (*3, 4, 15*), and protein concentrations were determined by quantitative amino acid analysis.
39. GroEL-6His, containing six histidine residues joined to the COOH-terminus of GroEL, was constructed by insertion mutagenesis and the polymerase chain reaction, followed by sequencing from the *groEL* gene obtained in plasmid pOF39 [O. Fayet, J. M. Louran, C. Georgopoulos, *Mol. Gen. Genet.* **202**, 435 (1986)]. His-tagged GroEL was purified from *E. coli* extracts by affinity chromatography on a $Ni^{2+}$-NTA column (Qiagen). GroEL-6His bound stably to $Ni^{2+}$-NTA in the absence and presence of nucleotide.
40. Unfolded rhodanese was diluted 100-fold from a solution containing 6 M GdmCl, 30 mM tris-HCl (pH 7.5), and 5 mM DTT into buffer A at 4°C by rapid mixing immediately before initiating injection into the BIAcore flow cell. This technique excludes the possibility of exposing the chaperonin complex to locally high concentrations of denaturant during the dilution step. The solution reached the flow cell after ~30 s. The $t_{1/2}$ for rhodanese aggregation was ~5 min. Allowing aggregation to occur before injection into the flow cell prevented the stimulatory effect of unfolded rhodanese on dissociation of GroEL:GroES.
41. We thank R. Granzow for critical support and discussion. Supported by NIH grant GM 50908.

4 April 1995; accepted 16 June 1995

# Growth of Tobacco Protoplasts Stimulated by Synthetic Lipo-Chitooligosaccharides

Horst Röhrig,* Jürgen Schmidt, Richard Walden, Inge Czaja, Edvins Miklaševičs, Ursula Wieneke, Jeff Schell, Michael John

**Nodulation (Nod) factors are lipo-chitooligosaccharides (LCOs) secreted by rhizobia to trigger the early steps of nodule organogenesis in leguminous plants. A method to synthesize LCOs in vitro was developed. Synthetic LCOs alleviated the requirement for auxin and cytokinin to sustain growth of cultured tobacco protoplasts. LCOs containing $C_{18:1}$ *trans*–fatty acyl substituents were more effective than those containing *cis*–fatty acids in promoting cell division as well as in activating an auxin-responsive promoter and the expression of a gene implicated in auxin action. These data indicate that LCOs redirect plant growth also in nonlegumes by activating developmental pathways also targeted by phytohormones.**

The basic structure of Nod factors produced by rhizobia consists of a β-1,4-linked *N*-acetylglucosamine (GlcNAc) containing tetra- or pentasaccharide, *N*-acylated with different long-chain fatty acids at the nonreducing glucosamine (GlcN) moiety (*1*, *2*). The role of LCOs as signaling molecules in plant development has stimulated interest in their synthesis. Recently, chemical synthesis of the alfalfa-specific Nod Rm-IV factor has been described (*3*). However, this strategy is relatively complex because of the large variety of functional groups requiring numerous coupling reactions, protection, and selective deprotection steps. We have now developed a simplified procedure for synthesis of LCOs. The acetyl group at the nonreducing GlcNAc residue is removed enzymatically from chitooligosaccharides by recombinant NodB (*4*), and a fatty acyl chain is then coupled chemically to the free amino group with fatty acid anhydrides as acylation agents (*5*). With this procedure, we *N*-acylated the tri-*N*-acetyl GlcN tetrasaccharide backbone with a saturated $C_{18}$ fatty acid, as well as with various monounsaturated $C_{18}$ fatty acids. The synthesized LCOs were biologically active, as confirmed by their ability to deform root hairs of vetch (*6*), a specific bioassay for Nod factors (*7*).

Separation of synthetic LCOs on a preparative $C_{18}$ reversed-phase high-performance liquid chromatography (HPLC) column (*8*) yielded two peaks corresponding to α and β anomers of the oligosaccharide backbone. The HPLC profile of an LCO, synthesized by *N*-acylation of the tetrasaccharide with *cis*-11-octadecenoic acid, that co-elutes with *Vicia*-specific NodRIv-IV ($C_{18:1}$) factor (*9*) is shown in Fig. 1A. To verify that the desired lipid had been attached to the tetrasaccharide, we released the corresponding fatty acid from the LCO by alkaline hydrolysis and subjected it to analysis by capillary gas-liquid chromatography (GLC) (*10*) (Fig. 1B). All fatty acids released from the synthetic LCOs by saponification co-chromatographed with authentic lipids. Radioisotopically labeled LCOs were hydrolyzed by chitinase to mono- and disaccharides (GlcNAc and $GlcNAc_2$) and lipid-linked di- or trisaccharides, which migrated on a thin-layer chromatography (TLC) plate faster than nondegraded LCOs (Fig. 1C) (*11*). Together, these results confirmed the presence of a β-1,4 linkage between GlcNAc residues in synthetic LCOs as well as of acyl substituents at the nonreducing terminus of the carbohydrate backbone.

In legumes, LCOs trigger the formation of the root nodule by initiating cell division at

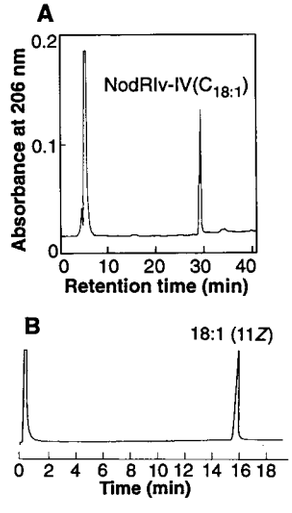


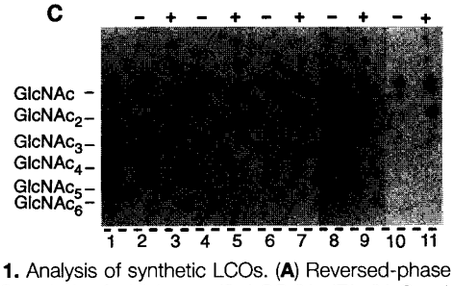


**Fig. 1.** Analysis of synthetic LCOs. (**A**) Reversed-phase HPLC analysis of a *Vicia*-specific LCO (NodRIv-IV, $C_{18:1}$) synthesized by *N*-acylation of tri-*N*-acetyl-GlcN tetrasaccharide with *cis*-11-octadecenoic acid. HPLC was performed as described (*8*). (**B**) Capillary GLC analysis of the fatty acid released from vaccenoylated tetrasaccharide by saponification (*10*): *cis*-11-octadecenoic acid [18:1 (11*Z*)]. (**C**) Thin-layer chromatography of products derived from the action of chitinase on *N*-acylated tri-*N*-[$^{14}$C]acetyl-β-1,4-D-GlcN tetrasaccharides (*11*). Samples (2 μl) were spotted on a silica gel 60 plate, which was then developed and subjected to autoradiography (*11*). Incubations were performed in the absence (–) or presence (+) of chitinase. Broken line, the origin of sample application. Lanes: 1, $^{14}$C-labeled GlcNAc to hexa-acetylchitohexaose ($GlcNAc_6$); 2 and 3, octadecanoylated tetrasaccharide; 4 and 5, *trans*-9-octadecenoylated tetrasaccharide; 6 and 7, *cis*-9-octadecenoylated tetrasaccharide; 8 and 9, *trans*-11-octadecenoylated tetrasaccharide; 10 and 11, *cis*-11-octadecenoylated tetrasaccharide.

Max-Planck-Institut für Züchtungsforschung, Carl-von-Linné-Weg 10, 50829 Köln, Germany.

*To whom correspondence should be addressed.